Zentrum für Technomathematik

Fachbereich 3 – Mathematik und Informatik

Evaluation of various phase-transition models for 100Cr6 for application in commercial FEM programs

Michael Böhm **Martin Hunkel**
Alfred Schmidt **Michael Wolff**

Report 02–14

Berichte aus der Technomathematik

Report 02–14 **Dezember 2002**

Michael Böhm, Martin Hunkel, Alfred Schmidt, and Michael Wolff

Evaluation of various phase-transition models for 100Cr6 for application in commercial FEM programs

Abstract. The numerical simulation of all steps of the production of a steel workpiece is nowadays a widely used tool for understanding and optimization of such processes. The transformation of austenite into ferritic phases is an important feature of heat treatment of steel. Good models for the non-isothermal phase transition are a necessary prerequisite for various other modeling steps. We evaluate some of the existing algorithms based on the isothermal Johnson-Mehl-Avrami model and compare their performance in the case of non-isothermal phase transitions with experimental data for steel 100Cr6 with exponential and linear cooling. The investigations presented here are part of a special research project on distortion engineering (SFB 570 at University of Bremen).

1. INTRODUCTION

The transformation of austenite into ferritic phases is an important feature of heat treatment of steel. In the literature various models for a large variety of cooling curves can be found. We consider here models based on the Johnson-Mehl-Avrami equation. While originally describing an isothermal transition, modifications exist for the description of the phase transition during a heating or cooling process. Commercial finite element packages for the simulation of problems with thermo-elasticity and -plasticity with phase transitions need such models for the description of the (then local) evolution of phase fraction distributions. Unfortunately, there is not yet a satisfactory model for a general cooling process, but parameters have to be adjusted for each special cooling. In practice, cooling curves might differ essentially from exponential ones. Oil-quenching serves as an example for this behaviour, where the heat-transfer coefficient exhibits a distinctive maximum at 400-600°C. In this article, we want to investigate the possibility to use adjusted parameters at least for a range of cooling conditions.

We evaluate some of the existing transformation models for steel 100Cr6 (SAE 52 100) under various cooling conditions. We want to consider here only the case of a single phase transition from austenite to pearlite, by restricting ourselves on the temperature range above 500°C. The transformation to martensite will not be considered here, because it is usually well described by the Koistinen-Marburger equation [8]. Further references can be found in [13, 14].

The investigations presented here are part of a special research project on distortion engineering (DFG grant SFB 570 at University of Bremen), where different production steps of steel workpieces are closely investigated for a number of model applications [4]. The steel considered here, 100Cr6, is one of two steels examined in the SFB research projects. Good models for non-isothermal phase transitions are a necessary prerequisite for various other modeling steps.

2. PHASE-TRANSFORMATION MODELS

The isothermal diffusion controlled transformation of austenite, e.g. formation of pearlite and bainite, can be well described by the Johnson-Mehl-Avrami (JMA) equation, introduced by Johnson and Mehl [7] and Avrami [1], which gives a formula for the average phase fraction $p(t)$ at time t,

$$p(t) = \bar{p}(T)\left(1 - \exp\left(-\Big(\frac{t}{\tau(T)}\Big)^{n(T)}\right)\right), \qquad t \geq 0. \tag{1}$$

Here, $\bar{p}$ is the equilibrium phase fraction (of pearlite, e.g.), τ is the time scale, and the exponent n determines the phase transition rate. All these parameters depend on the temperature T, where the phase transition takes place. For fixed T, these parameters can easily be determined, for example from isothermal dilatometer experiments, with a relatively high accuracy.

The same phase transition rates are described by the differential version of the JMA equation, an ordinary differential equation (ODE), where the transition rate does not explicitly depend on the time t but only on the current phase fraction $p(t)$

$$\begin{aligned} \dot{p}(t) &= F_{JMA}(p(t), T) \\ &= (\bar{p}(T) - p(t)) \frac{n(T)}{\tau(T)} \left(-\ln\left(1 - \frac{p(t)}{\bar{p}(T)}\right)\right)^{1-\frac{1}{n(T)}}, \qquad t \geq t_0, \\ p(t_0) &= p_0. \end{aligned} \tag{2}$$

For an arbitrary initial value $0 \leq p_0 < \bar{p}$, the solution of (2) fulfills $p(t) \in [0, \bar{p}]$ for all $t \geq t_0$. For $p_0 = 0$, the solution is constant $p(t) = 0$. A transition of phases is reached only for an initial value $p(t_0) = p_0 > 0$. A choice of $p(0)$ near 0 leads to a good approximation of the JMA solution (1).

On a large time scale, phase transition describes a relatively fast transition between two stationary states $p = 0$ and $p = \bar{p}$. Such a problem is called 'stiff', and special numerical methods are needed for a stable approximation of the solution, usually methods with implicit time discretization. Here, we are interested in a time scale, where not only the asymptotic behaviour but also the transition itself is accurately resolved. On this scale, where time steps of the discretization are small enough, also explicit methods are stable and can be used to solve the ODE problem. We use here the classical routines of Shampine and Gordon [11] for the solution of ODE initial value problems.

2.1 Models for non-isothermal phase transitions

While the JMA equation was originally derived to describe an isothermal transition, it is often also used for non-isothermal phase transitions in a cooling environment. Especially, commercial finite element packages employ this model. Besides that, different approaches exist which are not based on the JMA equation, for example by Leblond and Devaux [9], but will not be considered here.

The simplest possible treatment of the non-isothermal case just uses the differential JMA equation (2) with a given time dependent temperature $T(t)$,

$$\begin{aligned} \dot{p}(t) &= F_{JMA}(p(t), T(t)), \qquad t \geq t_0, \\ p(t_0) &= p_0, \end{aligned} \tag{3}$$

with temperature-dependent parameters $\bar{p}, \tau, n$ given from the corresponding isothermal transition. For very slowly changing temperatures, this approach describes reality relatively well.

A slight modification is needed in case when the equilibrium phase fraction $\bar{p}(T(t))$ may be decreasing in time. Then it may happen that the current phase fraction $p(t)$ is already larger than $\bar{p}(T(t))$, and the formula (3) does not make sense because the argument of the logarithm is negative. In this case, set $\dot{p}(t) = 0$. This choice is appropriate for a monotone phase transition in a decreasing temperature environment, where no inverse transition, back from pearlite to austenite, is possible.

A numerical method for the approximate solution of this problem was described by Hougardi and Yamazaki [5]. During small time steps, the temperature is considered locally constant, allowing the use of the explicit formula (1) for the solution on the small time interval. Thus, the method works even with an initial value $p_0 = 0$. When the time step size converges to zero, the solution of Hougardi's algorithm converges to the solution of equation (3). A modification of this algorithm, introduced by Denis [3], combines Hougardi's algorithm with Scheil's rule [10] for incubation, nucleation and initial growth of grains in a non-isothermal environment, by determining a time t_0 for the generation of an initial phase fraction $p_0 > 0$ by Scheil's rule, and using Hougardi's algorithm (and thus equation (3)) for time $t > t_0$.

Unfortunately, the simple approach (3) does not give satisfactory results in the case of high cooling rates. Experiments show that the transition rates are different than predicted by this model. In order to describe

such a situation in a phenomenological way, it is assumed that a more correct model for the non-isothermal phase transition is an ODE like

$$\dot{p}(t) = \tilde{F}(p(t), T(t), \dot{T}(t)). \tag{4}$$

with

$$\tilde{F}(p(t), T, 0) = F_{JMA}(p(t), T). \tag{5}$$

As such a function $\tilde{F}$ is not known explicitly, different multiplicative approaches for linearizations of $\tilde{F}$ around F_{JMA} are applied in order to get simple variations of the JMA equation. In the commercial finite element package SYSWELD [12], a linearization

$$\text{A:} \qquad \tilde{F}_1(p(t), T(t), \dot{T}(t)) = f(\dot{T}(t))\, F_{JMA}(p(t), T(t)) \tag{6}$$

can be used. For compatibility with (5), the condition $f(0) = 1$ follows. Hunkel et al. [6] introduced a linearization

$$\text{B:} \qquad \tilde{F}_2(p(t), T(t), \dot{T}(t)) = (1 - g(T(t))\dot{T}(t))\, F_{JMA}(p(t), T(t)). \tag{7}$$

For both approaches A and B, values of functions f or g are not known explicitly, but have to be determined by comparison with experimental data.

For a single cooling experiment with strictly monotone temperature $T(t)$ and cooling rate $\dot{T}(t)$ (like in the case of an exponential cooling), a one-to-one correspondence of time t and temperature (and cooling rate) is given. Thus, it would be possible to calculate values of f or g when the phase transition rate $\dot{p}(t)$ is known. Such a direct experimental evaluation of parameters is not possible when the cooling rates are not strictly monotone (for example in case of constant cooling), or when a model for the application to different cooling rates is needed.

Additionally, simple expressions with only few parameter values for f or g are most welcome, in order to compare functions for different (or a range of) coolings or even different materials.

3. EXPERIMENTAL DATA

We base our investigation on data from dilatometer experiments with exponential or linear cooling profiles. Data sets from the dilatometer consist of discrete times t_i and corresponding measured sample lengths L_i and temperature values T_i. The temperature is considered to be prescribed by the experimental setup, so the release of latent heat by phase transitions is neglected here. In order to derive experimental values of the phase fraction, we assume a linear mixing rule for the thermal expansion for pure austenite and pearlite materials. Let $L_A(T)$ and $L_P(T)$ denote the corresponding length of a sample of austenite or pearlite at temperature T, then the mixing assumption for a pearlite fraction p (and austenite fraction $1 - p$) reads

$$L(T) = pL_P(T) + (1 - p)L_A(T), \tag{8}$$

and the pearlite fraction can be calculated by

$$p = \frac{L(T) - L_A(T)}{L_P(T) - L_A(T)}. \tag{9}$$

For a purely thermo-elastic material without phase transitions, the length varies linearly with temperature changes by thermal expansion. Such a behaviour could be assumed for the pure phases austenite and pearlite, and the thermal expansion coefficient could be calculated from the experiments by investigating only the temperature ranges, where no phase transition takes place. Unfortunately, the experiments do not show a purely linear behaviour, and additionally do not give the same coefficients for different samples (of the same material). Thus, is is not possible to use a common coefficient for different experiments. Figure 1 shows relative length changes (in percentage of the initial sample length at room temperature) over temperature from two dilatometer experiments, together with 1st and 2nd order fits to the single phase thermal expansions. In the right part, the austenite phase fraction $1 - p$ is shown, evaluated as shown above with formula (9).

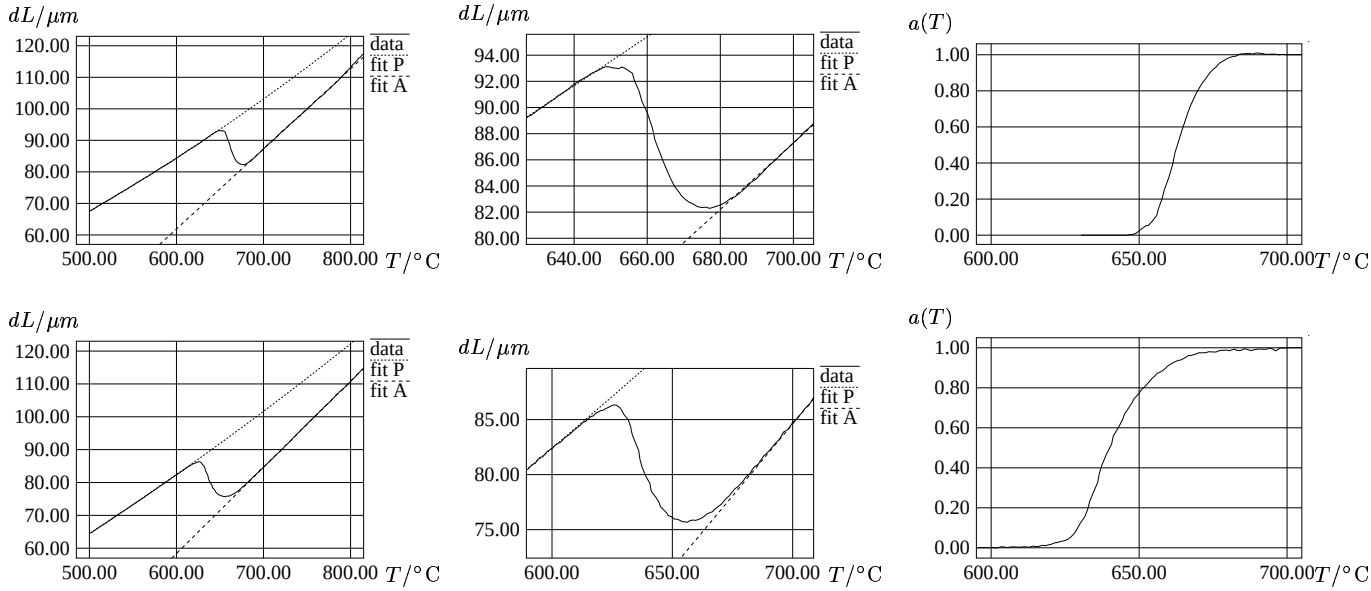

Figure 1: Data from two different dilatometer experiments with exponential cooling, $t_{850/100}$=1000s (top) and 500s (bottom). Left: Experimental expansion (measured in μm) over temperature (in $^\circ$C) and fits to pure pearlite and austenite expansions. Middle: Zoom to transition. Right: Austenite phase fraction over temperature.

Parameters $\tau(T)$ and $n(T)$ for the JMA equation were determined from isothermal dilatometer experiments with samples of the 100Cr6 steel under consideration. Usually, this can be done only for a few isothermal experiments with different temperatures, giving only a few discrete values of τ and n which have to be interpolated in an appropriate way. Here, we use a representation by functions

$$\tau(T) = \tau_0 \, \exp\Big(\frac{Q}{T}\Big) \exp\Big(\frac{P}{T(T_P - T)^2}\Big), \qquad n(T) = n_0 + n_1 T \quad \text{(piecewise)}, \tag{10}$$

with T in °K, where the numbers $\tau_0, P, Q, T_P, n_0, n_1$ were chosen to fit a set of isothermal experiments. The formula for τ reflects the idea that the time scale is reciprocally proportional to the density of nuclei and to the diffusion coefficient. In the essential temperature range between 580°C and 720°C, the parameters lead to an isothermal TTT diagram with 1% and 99% lines as shown in Figure 2.

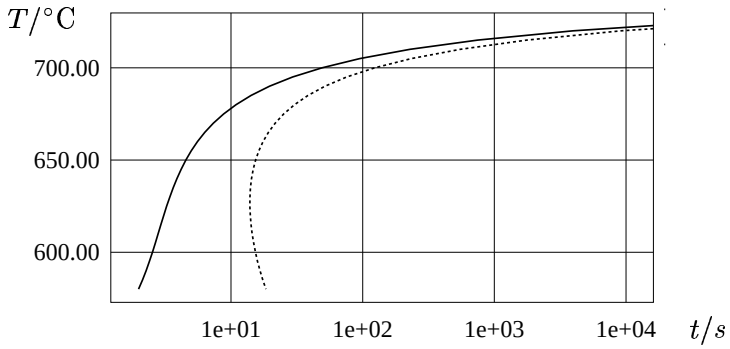

Figure 2: Isothermal TTT diagram with lines of 1% and 99% pearlite phase fraction.

4. RESULTS

We compare the experimental data with phase fractions calculated with five different models, the original time dependent JMA model (3) approximated with an ODE solver, Houagardi's discretization, Denis' model, and the two JMA modifications described above, model A (6), and model B (7).

For the two modified models A and B, the parameter functions $f(\dot{T})$ and $g(T)$ are generated by an optimization process over several experimental data sets. Both functions are given by interpolation of

discrete values $f(\dot{T}_i), i = 1, \ldots, N$ or $g(T_i), i = 1, \ldots, M$. These values are optimized such that the sum of squared errors between experimental and numerical phase fractions for relevant time intervals over the set of experiments is minimized. For the optimization, we use the classical minimization routines of Brent [2]. As such methods are only able to find local minima near the start point, some appropriate initial values have to be chosen by hand.

4.1 Exponential cooling

First, we present results for exponential cooling conditions. We consider four experimental data sets with coolings from $T = 850°\mathrm{C}$ to $T = 100°\mathrm{C}$ in $t_{850/100}$=2000s, 1000s, 500s, and 300s. These correspond to $t_{800/500}$ durations around 413s, 206s, 103s, and 62s. The corresponding austenite phase fraction curves over temperature are given in Figure 3 (because of different time scales, phase fraction curves over time would not give comparable information).

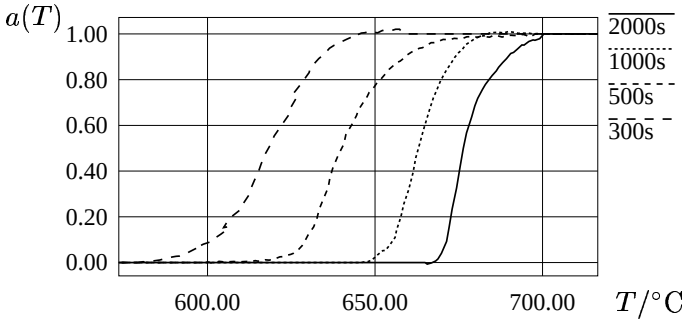

Figure 3: Experiments: Austenite phase fraction $a = 1 - p$ over temperature for four different exponential coolings with $t_{850/100}$=2000s, 1000s, 500s, and 300s.

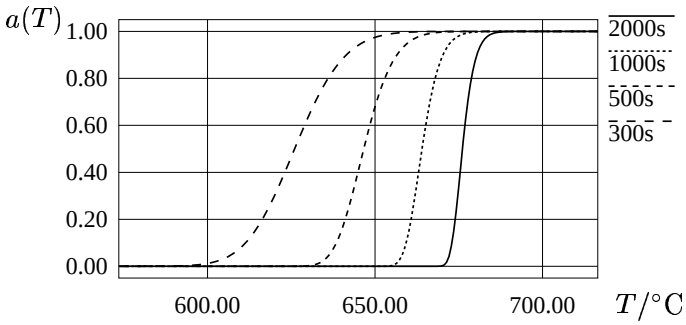

Figure 4: JMA model (3): Austenite phase fraction over temperature.

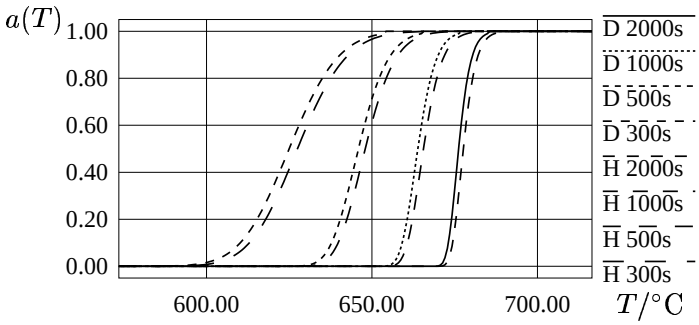

Figure 5: Denis' and Hougardi's models: Austenite phase fraction over temperature.

Without any correction, the JMA model (3) applied to the exponential temperature data leads to austenite fractions as shown in Figure 4. While the unmodified model is able to predict the general temperature range (and time) where the transition takes place, usually the experimental phase transitions start earlier than predicted, at higher temperatures, and finish later, at lower temperatures. Figure 5 shows results of Hougardi's and Denis' algorithms. As expected, Hougardi's discretization gives nearly the same result as a general ODE discretization. As the constant 'low' temperature $T(t_n)$ is used during the time

step $(t_n - 1, t_n)$, the transition starts a bit ahead of the ODE model. As result of using Scheil's rule for the incubation time, Denis' algorithm delays the transition for a short time, but then gives a similar shape for the transition profile like the JMA ODE model and Hougardi's algorithm. Mean square errors for the three approaches are listed in Table 1.

Table 1: JMA, Denis' and Hougardi's models: Mean square errors.

	2000s	1000s	500s	300s
JMA	0.03751	0.02709	0.06265	0.08768
Denis	0.03726	0.02678	0.05714	0.07918
Hougardi	0.03185	0.03731	0.07353	0.09983

A useful modification of the JMA model should increase the transition rate in the beginning and slow it down near the end of the phase transition. For model A this would mean that $f(\dot{T}) > 1$ during initial transition (while the cooling rate $|\dot{T}|$ is larger for an exponential cooling), and $f(\dot{T}) < 1$ for smaller $|\dot{T}|$. Similarly, for model B, $(1 - g(T)\dot{T}) > 1$ initially and $(1 - g(T)\dot{T}) < 1$ later, or, as $\dot{T} < 0$ during cooling, $g(T) > 0$ initially and $g(T) < 0$ later. When the optimization procedure is applied to a single experimental data set, it returns parameters as expected, at least generally speaking. As the cooling rates during the phase transition for the four experiments do not overlap, the f parameters are given on separate $\dot{T}$ intervals. On the other hand, the temperature ranges for g do overlap, as is clear from the previous pictures. Table 2 gives mean square errors for a reasonable small number of parameters (around 10) for each experiment. As expected, both models give similarly reduced errors. The experimental data from slowest cooling is especially hard to model. The left part of Figure 6 shows resulting austenite phase fractions for both models.

Table 2: Modified JMA models A and B, parameters optimized for single experiments. Mean square errors.

	2000s	1000s	500s	300s
Model A	0.01166	0.00174	0.01160	0.00441
Model B	0.01273	0.00287	0.00612	0.00385

Table 3: Modified JMA models A and B, parameters optimized for full set of experiments (first two lines), all but first (middle two lines) and two fastest experiments (bottom two lines). Mean square errors.

	2000s	1000s	500s	300s
Model A, opt 2000s-300s	0.02751	0.00785	0.01002	0.01011
Model B, opt 2000s-300s	0.03126	0.01983	0.01643	0.00779
Model A, opt 1000s-300s		0.00710	0.00999	0.00949
Model B, opt 1000s-300s		0.01966	0.01627	0.00652
Model A, opt 500s-300s			0.00966	0.00856
Model B, opt 500s-300s			0.01011	0.00680

Next, we try to derive a common set of optimized parameters for all four experiments, by minimizing the square errors over all four curves. We used 16 parameters values for model A and 15 parameters for model B. The right part of Figure 6 shows resulting austenite phase fractions. Again, especially the slowest cooling experiment is hard to model, see top two lines in Table 3. For the case that this experiment is not considered, but only the other three, results are shown in the middle two lines. Finally, when only the two fastest experiments are considered, results are shown in the bottom lines. For each reduced set of experiments, the optimization was started with initial values taken as the optimal ones from the optimization with one more experiment. We see that model A is always performing better, mainly because the cooling rates from different experiments separate, as mentioned before. Model B is performing worse, as temperature ranges for different experiments overlap. But model B is improving when less experiments are used, indicating the fact that optimal parameters for experiments with similar cooling rates do not differ very much.

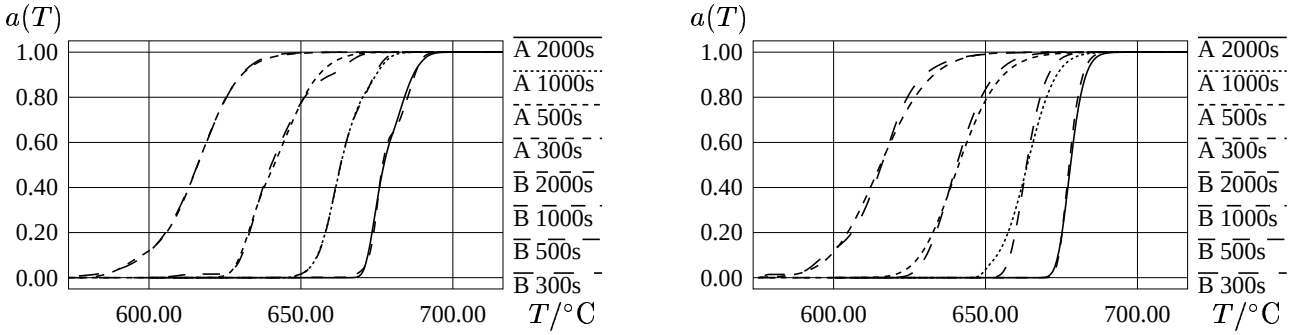

Figure 6: Modified JMA models A and B with separate parameter sets (left) and common parameter sets (right): Austenite phase fraction over temperature.

4.2 Linear cooling

Additional to the exponential cooling, we want to consider experiments with a constant cooling rate $\dot{T}$, which results in a linearly decreasing temperature over time. We use dilatometer data from three experiments with linear cooling from 850°C to 100°C in $t_{850/100}$=1000s, 500s, and 200s. Figure 7 shows the experimental austenite phase fraction over temperature, Figure 8 the results from simulations with the unmodified JMA model. Again, as in the case of exponential cooling, the results from Denis' and Hougardi's algorithms do not differ very much. Table 4 presents mean square errors from the three models in the top three rows.

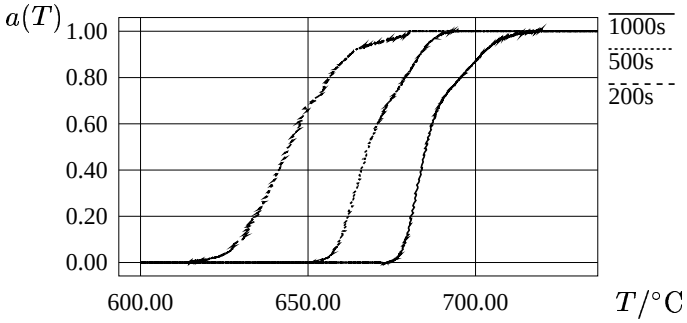

Figure 7: Experiments: Austenite phase fraction over temperature for three different linear coolings with $t_{850/100}$=2000s, 1000s, and 200s.

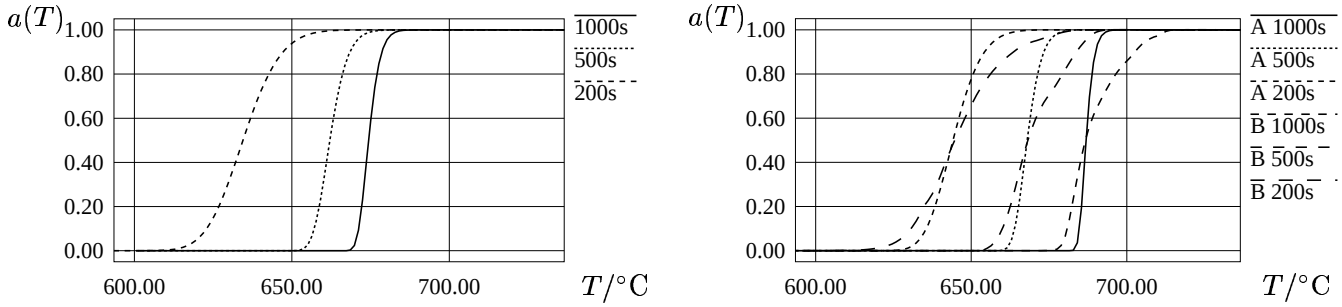

Figure 8: JMA model (left) and modified JMA models A and B with parameters optimized for single experiments (right): Austenite phase fraction over temperature for three different linear coolings.

Again, we try to optimize parameters for the two JMA modifications, models A and B. Now, for the linear temperature profiles, the cooling rates are constant for each experiment. As a consequence, there is only one free parameter $f(\dot{T})$ for model A for each experiment. For model B, the range of temperatures is similar to the one from exponential cooling. It is clear that model B should be able to approximate the experiments better, because of the availability of more free parameters. Mean square errors from both models are presented in the bottom half of Table 4.

Table 4: Various models: Mean square errors for linear cooling experiments. Middle lines: Modified JMA models A and B, separate parameters optimized for single experiments. Last line: Modified JMA model B, parameters optimized for all experiments.

	1000s	500s	200s
JMA	0.11457	0.05988	0.06710
Denis	0.10738	0.05266	0.06112
Hougardi	0.09112	0.03909	0.04484
Model A	0.03817	0.02153	0.01500
Model B	0.00310	0.00079	0.00166
Model B	0.08385	0.01351	0.00588

4.3 Summary

The results presented above show that the application of the "ordinary" JMA model to non-isothermal phase transition does not lead to good correspondence with experiments. The same holds for Denis' and Hougardi's algorithms. Modifications to the isothermal JMA model are necessary. Both modifications A and B are able to approximate single non-isothermal experiments quite well, especially in the case of an exponential cooling. For constant cooling rates, the results are not so well. Especially model A does not have enough degrees of freedom in order to handle such situations.

A more thorough investigation is needed for more general cooling situations, for example oil quenching, when the heat transfer coefficient varies substantially during the cooling process.

Acknowledgments

This work has been partially supported by DFG via the Sonderforschungsbereich "Distortion Engineering" (SFB 570), University of Bremen. Special thanks go to Stiftung Institut für Werkstofftechnik for the experimental data.

References

1. M. Avrami, J. Chem. Phys. 8 (1949) 212-224.
2. R.P. Brent, *Algorithms for minimization without derivatives* (Prentice-Hall 1973).
3. S. Denis, in *CISM courses and lectures - No 368, Mechanics of solids with phase changes*, edited by M. Bergveiller, F.D. Fischer (Springer-Verlag 1997).
4. F. Hoffmann, O. Keßler, T. Lübben, P. Mayr, HTM 57 (2002) 213-217.
5. H.P. Hougardy, K. Yamazaki, Steel Research 57 (1986).
6. M. Hunkel, T. Lübben, F. Hoffmann, P. Mayr, HTM 54 (1999) 365-372.
7. W.A. Johnson and R.F. Mehl, Trans. AIME 135 (1939) 416-458.
8. D.P. Koistinen, R.E. Marburger, Acta metall. 7 (1959) 59-60.
9. J.B. Leblond, J. Devaux, Acta Met. 32 (1984) 137-146.
10. E. Scheil, Archiv des Eisenhüttenwesens (1935) 565-567.
11. L.F. Shampine, M.K. Gordon, *Computer solution of ordinary differential equations. The initial value problem* (W.H. Freeman & Comp. 1975).
12. SYSWELD (TM) (2000).
13. M. Wolff, M. Böhm, E. Bänsch, D. Davis, Berichte aus der Technomathematik 00-07, FB 3, Universität Bremen (2000).
14. M. Wolff, M. Böhm, to appear in Technische Mechanik.

Berichte aus der Technomathematik ISSN 1435-7968

http://www.math.uni-bremen.de/zetem/berichte.html

— Vertrieb durch den Autor —

Reports **Stand: 7. Februar 2003**

98–01. Peter Benner, Heike Faßbender:
An Implicitly Restarted Symplectic Lanczos Method for the Symplectic Eigenvalue Problem, Juli 1998.

98–02. Heike Faßbender:
Sliding Window Schemes for Discrete Least-Squares Approximation by Trigonometric Polynomials, Juli 1998.

98–03. Peter Benner, Maribel Castillo, Enrique S. Quintana-Ortí:
Parallel Partial Stabilizing Algorithms for Large Linear Control Systems, Juli 1998.

98–04. Peter Benner:
Computational Methods for Linear–Quadratic Optimization, August 1998.

98–05. Peter Benner, Ralph Byers, Enrique S. Quintana-Ortí, Gregorio Quintana-Ortí:
Solving Algebraic Riccati Equations on Parallel Computers Using Newton's Method with Exact Line Search, August 1998.

98–06. Lars Grüne, Fabian Wirth:
On the rate of convergence of infinite horizon discounted optimal value functions, November 1998.

98–07. Peter Benner, Volker Mehrmann, Hongguo Xu:
A Note on the Numerical Solution of Complex Hamiltonian and Skew-Hamiltonian Eigenvalue Problems, November 1998.

98–08. Eberhard Bänsch, Burkhard Höhn:
Numerical simulation of a silicon floating zone with a free capillary surface, Dezember 1998.

99–01. Heike Faßbender:
The Parameterized SR Algorithm for Symplectic (Butterfly) Matrices, Februar 1999.

99–02. Heike Faßbender:
Error Analysis of the symplectic Lanczos Method for the symplectic Eigenvalue Problem, März 1999.

99–03. Eberhard Bänsch, Alfred Schmidt:
Simulation of dendritic crystal growth with thermal convection, März 1999.

99–04. Eberhard Bänsch:
Finite element discretization of the Navier-Stokes equations with a free capillary surface, März 1999.

99–05. Peter Benner:
Mathematik in der Berufspraxis, Juli 1999.

99–06. Andrew D.B. Paice, Fabian R. Wirth:
Robustness of nonlinear systems and their domains of attraction, August 1999.

99–07. Peter Benner, Enrique S. Quintana-Ortí, Gregorio Quintana-Ortí:
Balanced Truncation Model Reduction of Large-Scale Dense Systems on Parallel Computers, September 1999.

99–08. Ronald Stöver:
Collocation methods for solving linear differential-algebraic boundary value problems, September 1999.

99–09. Huseyin Akcay:
Modelling with Orthonormal Basis Functions, September 1999.

99–10. Heike Faßbender, D. Steven Mackey, Niloufer Mackey:
Hamilton and Jacobi come full circle: Jacobi algorithms for structured Hamiltonian eigenproblems, Oktober 1999.

99–11. Peter Benner, Vincente Hernández, Antonio Pastor:
On the Kleinman Iteration for Nonstabilizable System, Oktober 1999.

99–12. Peter Benner, Heike Faßbender:
A Hybrid Method for the Numerical Solution of Discrete-Time Algebraic Riccati Equations, November 1999.

99–13. Peter Benner, Enrique S. Quintana-Ortí, Gregorio Quintana-Ortí:
Numerical Solution of Schur Stable Linear Matrix Equations on Multicomputers, November 1999.

99–14. Eberhard Bänsch, Karol Mikula:
Adaptivity in 3D Image Processing, Dezember 1999.

00–01. Peter Benner, Volker Mehrmann, Hongguo Xu:
Perturbation Analysis for the Eigenvalue Problem of a Formal Product of Matrices, Januar 2000.

00–02. Ziping Huang:
Finite Element Method for Mixed Problems with Penalty, Januar 2000.

00–03. Gianfrancesco Martinico:
Recursive mesh refinement in 3D, Februar 2000.

00–04. Eberhard Bänsch, Christoph Egbers, Oliver Meincke, Nicoleta Scurtu:
Taylor-Couette System with Asymmetric Boundary Conditions, Februar 2000.

00–05. Peter Benner:
Symplectic Balancing of Hamiltonian Matrices, Februar 2000.

00–06. Fabio Camilli, Lars Grüne, Fabian Wirth:
A regularization of Zubov's equation for robust domains of attraction, März 2000.

00–07. Michael Wolff, Eberhard Bänsch, Michael Böhm, Dominic Davis:
Modellierung der Abkühlung von Stahlbrammen, März 2000.

00–08. Stephan Dahlke, Peter Maaß, Gerd Teschke:
Interpolating Scaling Functions with Duals, April 2000.

00–09. Jochen Behrens, Fabian Wirth:
A globalization procedure for locally stabilizing controllers, Mai 2000.

00–10. Peter Maaß, Gerd Teschke, Werner Willmann, Günter Wollmann:
Detection and Classification of Material Attributes – A Practical Application of Wavelet Analysis, Mai 2000.

00–11. Stefan Boschert, Alfred Schmidt, Kunibert G. Siebert, Eberhard Bänsch, Klaus-Werner Benz, Gerhard Dziuk, Thomas Kaiser:
Simulation of Industrial Crystal Growth by the Vertical Bridgman Method, Mai 2000.

00–12. Volker Lehmann, Gerd Teschke:
Wavelet Based Methods for Improved Wind Profiler Signal Processing, Mai 2000.

00–13. Stephan Dahlke, Peter Maass:
A Note on Interpolating Scaling Functions, August 2000.

00–14. Ronny Ramlau, Rolf Clackdoyle, Frédéric Noo, Girish Bal:
Accurate Attenuation Correction in SPECT Imaging using Optimization of Bilinear Functions and Assuming an Unknown Spatially-Varying Attenuation Distribution, September 2000.

00–15. Peter Kunkel, Ronald Stöver:
Symmetric collocation methods for linear differential-algebraic boundary value problems, September 2000.

00–16. Fabian Wirth:
The generalized spectral radius and extremal norms, Oktober 2000.

00–17. Frank Stenger, Ahmad Reza Naghsh-Nilchi, Jenny Niebsch, Ronny Ramlau:
A unified approach to the approximate solution of PDE, November 2000.

00–18. Peter Benner, Enrique S. Quintana-Ortí, Gregorio Quintana-Ortí:
Parallel algorithms for model reduction of discrete–time systems, Dezember 2000.

00–19. Ronny Ramlau:
A steepest descent algorithm for the global minimization of Tikhonov–Phillips functional, Dezember 2000.

01–01. Efficient methods in hyperthermia treatment planning:
Torsten Köhler, Peter Maass, Peter Wust, Martin Seebass, Januar 2001.

01–02. Parallel Algorithms for LQ Optimal Control of Discrete-Time Periodic Linear Systems:
Peter Benner, Ralph Byers, Rafael Mayo, Enrique S. Quintana-Ortí, Vicente Hernández, Februar 2001.

01–03. Peter Benner, Enrique S. Quintana-Ortí, Gregorio Quintana-Ortí:
Efficient Numerical Algorithms for Balanced Stochastic Truncation, März 2001.

01–04. Peter Benner, Maribel Castillo, Enrique S. Quintana-Ortí:
Partial Stabilization of Large-Scale Discrete-Time Linear Control Systems, März 2001.

01–05. Stephan Dahlke:
Besov Regularity for Edge Singularities in Polyhedral Domains, Mai 2001.

01–06. Fabian Wirth:
A linearization principle for robustness with respect to time-varying perturbations, Mai 2001.

01–07. Stephan Dahlke, Wolfgang Dahmen, Karsten Urban:
Adaptive Wavelet Methods for Saddle Point Problems - Optimal Convergence Rates, Juli 2001.

01–08. Ronny Ramlau:
Morozov's Discrepancy Principle for Tikhonov regularization of nonlinear operators, Juli 2001.

01–09. Michael Wolff:
Einführung des Drucks für die instationären Stokes–Gleichungen mittels der Methode von Kaplan, Juli 2001.

01–10. Stephan Dahlke, Peter Maaß, Gerd Teschke:
Reconstruction of Reflectivity Desities by Wavelet Transforms, August 2001.

01–11. Stephan Dahlke:
Besov Regularity for the Neumann Problem, August 2001.

01–12. Bernard Haasdonk, Mario Ohlberger, Martin Rumpf, Alfred Schmidt, Kunibert G. Siebert:
h–p–Multiresolution Visualization of Adaptive Finite Element Simulations, Oktober 2001.

01–13. Stephan Dahlke, Gabriele Steidl, Gerd Teschke:
Coorbit Spaces and Banach Frames on Homogeneous Spaces with Applications to Analyzing Functions on Spheres, August 2001.

02–01. Michael Wolff, Michael Böhm:
Zur Modellierung der Thermoelasto-Plastizität mit Phasenumwandlungen bei Stählen sowie der Umwandlungsplastizität, Februar 2002.

02–02. Stephan Dahlke, Peter Maaß:
An Outline of Adaptive Wavelet Galerkin Methods for Tikhonov Regularization of Inverse Parabolic Problems, April 2002.

02–03. Alfred Schmidt:
A Multi-Mesh Finite Element Method for Phase Field Simulations, April 2002.

02–04. Sergey N. Dachkovski, Michael Böhm:
A Note on Finite Thermoplasticity with Phase Changes, Juli 2002.

02–05. Michael Wolff, Michael Böhm:
Phasenumwandlungen und Umwandlungsplastizität bei Stählen im Konzept der Thermoelasto-Plastizität, Juli 2002.

02–06. Gerd Teschke:
Construction of Generalized Uncertainty Principles and Wavelets in Anisotropic Sobolev Spaces, August 2002.

02–07. Ronny Ramlau:
TIGRA – an iterative algorithm for regularizing nonlinear ill–posed problems, August 2002.

02–08. Michael Lukaschewitsch, Peter Maaß, Michael Pidcock:
Tikhonov regularization for Electrical Impedance Tomography on unbounded domains, Oktober 2002.

02–09. Volker Dicken, Peter Maaß, Ingo Menz, Jenny Niebsch, Ronny Ramlau:
Inverse Unwuchtidentifikation an Flugtriebwerken mit Quetschöldämpfern, Oktober 2002.

02–10. Torsten Köhler, Peter Maaß, Jan Kalden:
Time-series forecasting for total volume data and charge back data, November 2002.

02–11. Angelika Bunse-Gerstner:
A Short Introduction to Iterative Methods for Large Linear Systems, November 2002.

02–12. Peter Kunkel, Volker Mehrmann, Ronald Stöver:
Symmetric Collocation for Unstructured Nonlinear Differential-Algebraic Equations of Arbitrary Index, November 2002.

02–13. Michael Wolff:
Ringvorlesung: Distortion Engineering 2
Kontinuumsmechanische Modellierung des Materialverhaltens von Stahl unter Berücksichtigung von Phasenumwandlungen, Dezember 2002.

02–14. Michael Böhm, Martin Hunkel, Alfred Schmidt, Michael Wolff:
Evaluation of various phase-transition models for 100Cr6 for application in commercial FEM programs, Dezember 2002.